Coherent optical time domain relectometry: The theoretical basis for distributed acoustic sensing technologies

Matt Eaid and Kris Innanen

ABSTRACT

The applications of distributed acoustic sensing (DAS) fibres for seismic acquisition, reservoir monitoring, and smart city applications continues to expand. As the interest in utilizing optical fibres for seismic acquisition continues to grow, it becomes increasingly important to understand the underlying technology that makes them effective. Understanding the theoretical means by which DAS fibres acquire seismic data allows for an improved understanding of their limitations and opportunities, and permits better decision making in how they are deployed. A grasp of the theory behind DAS technology also aids in the interpretation of the data, and trouble shooting when challenges arise. The way in which a given interrogator unit converts disturbances along the fibre to seismic strain varies and is typically proprietary. However, most implementations are based on a variant of coherent optical time domain reflectometry (COTDR), a technology used by telecommunications companies to detect flaws in installed optical fibres. In this short note we cover the topic of COTDR and discuss how it has been adapted for use in the acquisition of strain data resulting from seismic wave propagation.

INTRODUCTION

The backscattering of light in optical fibres due to microscopic inhomogeneities in the refractive index is a well known problem in the telecommunications industry. Typically treated as a source of noise, telecommunication service companies employ devices known as Optical Time domain Reflectometers (OTDR), exploiting the backscattered light to test the fibre quality and detect flaws with splices and coupling. Recent work has focused on using the interference pattern of the backscattered light, within in an interferometric framework to turn the fibres into sensors of physical quantities including strain, stress, temperature, and fibre rotation. For this to be achieved, the laser pulse injected into the fibre must be fairly coherent, a condition not met by typical OTDR. Special reflectometers, known as Coherent Optical Time Domain Reflectometers (COTDR) have been developed to turn standard optical fibres into highly sensitive, distributed strain senors. These sensors have exploded in popularity finding applications in aerospace, perimeter defense, military, smart-city sensing, and oil and gas. This short note conveys the ideas behind the physical basis for distributed fibre sensors, and discusses special considerations for oil and gas strain sensing.

RAYLEIGH SCATTERING IN OPTICAL FIBRES AND THE ROLE OF BACKSCATTERED LIGHT

Rayleigh scattering of an injected laser pulse in silica glass is a well known phenomenon that has been a burden on long range fibre deployment for the telecommunications industry for a long time. As the laser pulse traverses the fiber it scatters as it interacts with microscopic fluctuations in the refractive index, that are a consequence of the fibre drawing process. Research has focused on developing varying synthesizing procedures to develop a more homogeneous silica glass that reduces scattering, however, all fibres made to date still suffer from some scattering (Sakagucki and Todoroki, 1996).

The idiom one persons noise is another persons signal rings true. Not long after the development of optical fibres, work began to exploit the backscattered light to provide information about the conditions of the medium in which the fibre is placed. Figure 1 shows the basic setup of an early device aimed at recording and interrogating the backscattered signal (Shatalin et al., 1998). It is assumed that a coherent optical pulse, $\epsilon(t)$, is launched into a single mode optical fibre of length L with a distributed reflectivity profile $r(z)$, caused by changes in the refractive index. An external perturbation, which can take the form of strain, stress, or temperature variation, occurs at a distance z_0. The disturbance leads to a phase modulation of ϕ in the backscattered light. Assuming Rayleigh scattering, the backscattered light from the portion of the fibre between the interrogator and z_0 will return with the same phase as the emitted laser pulse. Light returning from portions of the fibre after z_0 will have a phase that has been modulated by the external stressor.

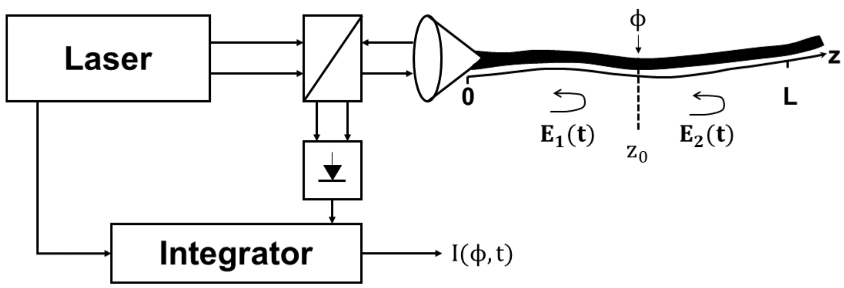

FIG. 1. Early interrogator setup from Shatalin et al. (1998)

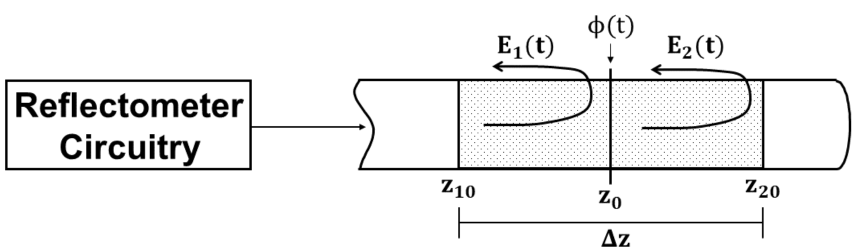

FIG. 2. Zoom in of a portion of the fibre in figure 1 leading to strong interference, modified from Mamedov et al. (1994)

.

Now consider a potion of the fibre such that the path difference between backscattered pulses $\mathbf{E_1(t)}$ and $\mathbf{E_2(t)}$ is smaller than the coherence length of the laser such that strong interference occurs in the backscattered light as shown in figure 2. When this condition is satisfied the electric field $\mathbf{E}(\phi, t)$ returning to the launch end of the fibre is a superposition of the unmodulated and modulated signals,

$$\mathbf{E}(\phi, t) = \mathbf{E_1}(t) + \mathbf{E_2}(t)e^{2i\phi(t)} \tag{1}$$

where $\mathbf{E_1}(t)$ and $\mathbf{E_2}(t)$ are themselves complex signals given by,

$$\mathbf{E_1}(t) = \int_{z_{10}}^{z_0} \epsilon(t - 2z/v) r(z) e^{-2i\beta z} dz \tag{2}$$

$$\mathbf{E_2}(t) = \int_{z_0}^{z_{20}} \epsilon(t - 2z/v) r(z) e^{-2i\beta z} dz \tag{3}$$

.

where $2z/v$ is the group delay, and $2\beta z$ is the phase delay with β being the wave propagation constant, and z_{10} and z_{20} are chosen as the boundaries of the distance over which $\mathbf{E_1}(t)$ and $\mathbf{E_2}(t)$ will interfere coherently.

The optical wave intensity at the optical time domain reflectometer is found from the square of the amplitude (intensity) of the electric field,

$$\begin{aligned} I(\phi, t) = |\mathbf{E}(\phi, t)|^2 = \mathbf{E}\mathbf{E}^* &= \left(\mathbf{E_1}(t) + \mathbf{E_2}(t) e^{i2\phi}\right)\left(\mathbf{E_1^*}(t) + \mathbf{E_2^*}(t) e^{-i2\phi}\right) \\ &= I_1(t) + I_2(t) + \sqrt{I_1(t) I_2(t)} \left(e^{i(\phi_2 - \phi_1 + 2\phi)} + e^{-i(\phi_2 - \phi_1 + 2\phi)}\right) \\ &= I_1(t) + I_2(t) + 2\sqrt{I_1(t) I_2(t)} \cos(2\phi + \phi_0) \end{aligned} \tag{4}$$

where,

$$\phi_0 = \phi_2 - \phi_1 = \arg(\mathbf{E_2}) - \arg(\mathbf{E_1})$$

Equation (4) represents the intensity for the interference of two coherent beams, where the last term provides information about the interference, and is a function of the phase modulation ϕ. The intensity in equation (4) can be re-written as,

$$I(\phi, t) = I_0(t)[1 + V(t) \cos(2\phi + \phi_0)] \tag{5}$$

with,

$$I_0 = I_1(t) + I_2(t) \tag{6}$$

and,

$$V(t) = \frac{2\sqrt{I_1(t) I_2(t}}{I_1(t) + I_2(t)}. \tag{7}$$

The term $V(t)$ is known as the fringe visibility, a term quantifying the contrast of the interference. In optical interferometers it is also a measure of the level of coherence of two signals. Shatalin et al. (1998) shows that for the geometries in figures 1 and 2 the visibility may be written as,

$$V(t) = \left[1 - \left(\frac{vt - 2z_0}{\Delta z}\right)^2\right]^{1/2} \tag{8}$$

which is real only when the following inequality is satisfied,

$$z_0 - \frac{\Delta z}{2} < \frac{vt}{2} < z_0 + \frac{\Delta z}{2} \tag{9}$$

showing that the interference is only visible, in other words the two reflected pulses coherently interfere, only for a distance equal to the spatial resolution interval centered around the point of the phase modulation.

MACH-ZEHNDER INTERFEROMETERY IN DISTRIBUTED SENSORS

Mach-Zehnder interferometers are primarily used to measure changes in the pressure, temperature, or density in fluids. This is achieved by measuring the interference pattern on two different detectors between a reference beam and a beam that has passed through the sample as shown in figure 3.

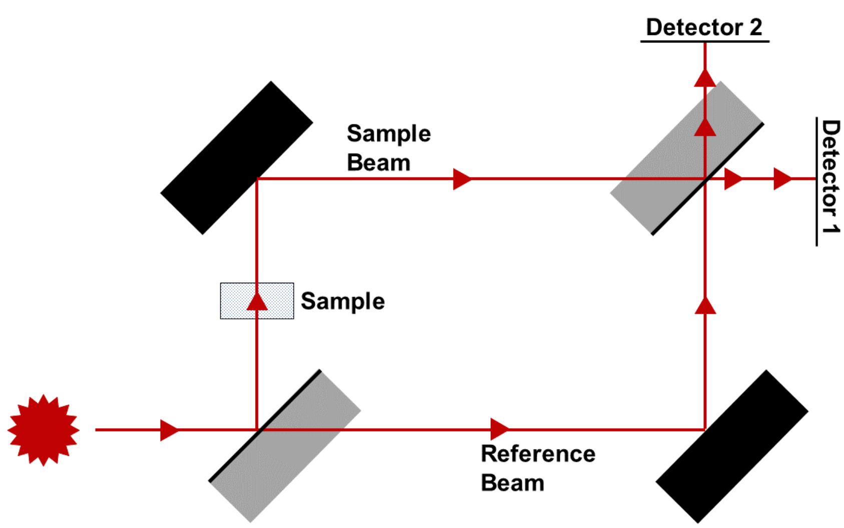

FIG. 3. Schematic diagram of the general layout for a Mach-Zehnder interferometer. The black boxes represent standard mirrors, while the grey boxes represent half silvered mirrors with the reflecting edge highlighted in black.

The Mach-Zehnder interferometer (MZI) works by employing half silvered mirrors which split the beam, reflecting half of the light, while allowing half of the light to transmit. This causes the single beam entering the interferometer to split into two beams, one of which passes through the sample under investigation and is called the sample beam. The other beam is known as the reference beam. Both beams are the directed towards two detectors by carefully oriented mirrors. Before reaching the detectors, each beam passes through another half silvered mirror further splitting each beam so that an interference pattern is produced on each detector. In the absence of a sample the beams arriving at detector one are perfectly in phase causing constructive interference while the beams at detector two are perfectly out of phase leading to total destructive interference and the absence of a signal at detector two. The presence of a sample induces a phase modulation in the sample beam, leading to partial constructive interference at each detector, altering the interference patterns. The change in the interference pattern can be utilized to infer properties of the sample. In distributed acoustic sensors, the MZI lacks a conventional sample, and the phase modulations are instead produced by strain disturbances along the fibre.

An unbalanced Mach-Zehnder interferometer has two arms that differ in length. The longer arm delays the signal from the closer portion of the fibre. This allows for the coherent interference of the light scattering from different parts of the fibre separated by a distance known as the gauge length, where the gauge length is equal to half the delay length of the interferometer as shown in figure 4. In the case of seismic strain recording, more than one phase modulation can occur over the gauge length, resulting in an interference pattern that is a function of the average phase modulation. Longer gauge lengths increase the sensitivity by summing over more phase modulations, but reduces the resolution.

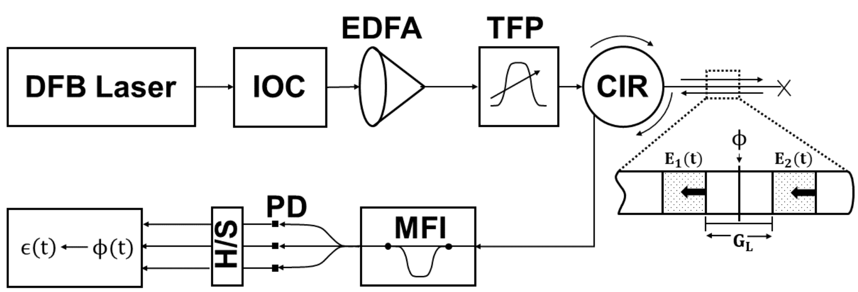

FIG. 4. Modern interrogator circuitry. The laser is modulated by an integrated optical chip (IOC), then amplified by an erbium doped amplifier EDFA) and filtered for noise by a tunable Fabry-Perot filter (TFP). The pulse then enters an optical circulator (CIR) which transmits it to the fibre. The backscattered signal is delayed by the Mach-Zehnder interferometer (MZI) and split to three photodiodes (PD). The return signal is then gated to analyze varying portions of the fibre. Modified from Posey Jr. et al. (2000)

.

A challenge with early optical time domain reflectometers is that they only provide information that a change in the backscattered intensity has occured and the location along the fibre for phase modulation causing the intensity perturbation. To gather information about conditions of the medium in which the fibre is placed it would be more useful to obtain values of the phase modulation that altered the intensity pattern. To achieve this Posey Jr. et al. (2000) present the more complex circuitry shown in figure 4. As the laser exits the interferometer it enters a 3x3 coupler and is split into three components, each of which interacts with a photo diode converting the light into an electrical signal. The coupler is designed such that each diode receives a signal that is 120 degrees out of phase with the signals at the other two couplers (Todd et al., 1999).

The voltage at each photo diode is then given as,

$$V_n = C_n + A_n \cos\big(\phi(t) + 2\pi/3(n-1)\big) \tag{10}$$

resulting in,

$$\begin{aligned} V_1 &= C_1 + A_1 \cos(\phi(t)) \\ V_2 &= C_2 + A_2 \cos(\phi(t) + 2\pi/3) \\ V_3 &= C_3 + A_3 \cos(\phi(t) + 4\pi/3). \end{aligned}$$

The constants A_n and C_n can be affected by fluctuations in the source intensity. It is more useful to employ relative constants that are not affected by source fluctuations but instead are a function of the geometric layout. This can be achieved using the relations $C = C_1, A = A_1$, and $\alpha_n = C_n/C_1 = A_n/A_1$ (Todd et al., 1999). The voltage at each diode is then given by,

$$\begin{aligned} V_1 &= C + A\cos(\phi(t)) \\ V_2 &= \alpha_2\bigg[C + A\bigg\{\frac{-\cos\phi(t)}{2} + \frac{\sqrt{3}\sin\phi(t)}{2}\bigg\}\bigg] \\ V_3 &= \alpha_3\bigg[C + A\bigg\{\frac{-\cos\phi(t)}{2} - \frac{\sqrt{3}\sin\phi(t)}{2}\bigg\}\bigg] \\ &. \end{aligned}$$

These voltages can be used to compute the phase modulation by first multiplying V_1 by $\alpha_2\alpha_3$, V_2 by α_3, and V_3 by α_2 and then subtracting $2V_1$ from $V_2 + V_3$,

$$\cos\phi(t) = -\frac{\alpha_3 V_2 + \alpha_2 V_3 - 2\alpha_2\alpha_3 V_1}{3A\alpha_2\alpha_3}. \tag{11}$$

Subtracting $\alpha_2 V_3$ from $\alpha_3 V_2$ provides,

$$\sin\phi(t) = \frac{\alpha_3 V_2 - \alpha_2 V_3}{\sqrt{3}A\alpha_2\alpha_3}. \tag{12}$$

Dividing equation (12) by equation (11) gives an expression for the tangent of the phase modulation,

$$\tan\phi(t) = -\sqrt{3}\frac{\alpha_3 V_2 - \alpha_2 V_3}{\alpha_3 V_2 + \alpha_2 V_3 - 2\alpha_2\alpha_3 V_1}. \tag{13}$$

The coupler thus provides a means of computing the phase modulation that induced the fluctuation in the intensity pattern. This process is known as demodulation and provides a method for estimating a physical perturbation of the optical fibre that lead to a given phase modulation. Empirical measurements of the phase modulation can be made in a lab for a known strain perturbation. In field the, phase modulations can be compared against empirical values to estimate the strain in the host rock. This process makes optical fibres powerful tools for distributed sensing. Theoretically every point along the fibre can be used as a sensor for perturbations in the physical medium the fibre is placed in. Far reaching applications for these type of sensors have been found in aerospace, defense, infrastructure health, oil and gas, perimeter security, and smart city applications. As the technology, and research in the field of distributed sensors progresses, optical fibres hold the potential to be the sensor of choice in the future. They have become a popular tool for seismic data acquisition in VSP surveys, reservoir monitoring, and high resolution parameter estimation.

CONCLUSIONS

This brief note provides an introduction to the underlying technology behind DAS fibre technology. While it does not provide an exhaustive coverage of the entire field of optical time domain reflectometry, its purpose is to give a brief coverage of their basic principles to make DAS research more accessible. Strides continue to be made in better interrogator circuitry, reduced gauge lengths, and engineered fibres that have impurities etched into them at periodic intervals. While improvements to the fibre technologies expand the capabilities of DAS technologies, the underlying principles remain similar to those presented here.

ACKNOWLEDGMENTS

The authors would like to thank the sponsors of the CREWES project as well NSERC under the grant CRDPJ 461179-13 for making this work possible through their financial support.

REFERENCES

Mamedov, A., Potapov, V., and Shatalin, S., 1994, Interferometry with Rayleigh backscattering in a single-mode optical fibre: Optics Letters, **19**, No. 3.

Posey Jr., R., Johnson, G., and Vohra, S., 2000, Strain sensing based on coherent Rayleigh scattering in an optical fibre: IEE Electronics Letters, **36**, No. 20.

Sakagucki, S., and Todoroki, S., 1996, Rayleigh scattering in silica glass: Journal of the American Ceramic Society, **79**, No. 11.

Shatalin, S., Treschikov, V., and Rogers, A., 1998, Interferometric optical time-domain reflectometry for distributed optical-fiber sensing: Applied Optics, **37**, No. 24.

Todd, M., Johnson, G., and Chang, C., 1999, Passive, light intensity-independent interferometric merthod for fibre Bragg grating interrogation: IEE Electronics Letters, **35**, No. 22.